

CONVEX BACKSCATTERING SUPPORT IN ELECTRIC IMPEDANCE TOMOGRAPHY

MARTIN HANKE*, NUUTTI HYVÖNEN†, AND STEFANIE REUSSWIG‡

Abstract. This paper reinvestigates a recently introduced notion of backscattering for the inverse obstacle problem in impedance tomography. Under mild restrictions on the topological properties of the obstacles it is shown that the corresponding backscatter data are the boundary values of a function that is holomorphic in the exterior of the obstacle(s), which allows to reformulate the obstacle problem as an inverse source problem for the Laplace equation. For general obstacles the convex backscattering support is then defined to be the smallest convex set that carries an admissible source, i.e., a source that yields the given (backscatter) data as the trace of the associated potential. The convex backscattering support can be computed numerically; numerical reconstructions are included to illustrate the viability of the method.

Key words. Electric impedance tomography, inclusions, backscattering, backscattering support, source support

AMS subject classifications. 35R30, 65N21

1. Introduction. The inverse obstacle problem in electric impedance tomography consists in the reconstruction of an unknown inclusion (an insulating obstacle, say) in some object of known homogeneous conductivity from electrostatic measurements at the boundary of the object. Appropriate measurements are, for example, the electrostatic potential at the boundary of the object when a certain current is injected through the boundary into the object. Depending on the physical properties of the inclusion and on the number of boundary currents to which the object is exposed, different numerical methods can be applied to reconstruct the inclusion, cf., e.g., [1, 2, 6, 8, 12, 16, 17, 19, 21, 24].

In this paper we consider the (two-dimensional) inverse obstacle problem with a nonstandard set of data that has been introduced and termed *backscatter data* recently in [9]: A pair of electrodes is used to drive a given current and record the resulting voltage while being rotated around the object. The notion ‘backscattering’ has been adopted for this setup because of the relation to the ‘usual’ backscattering of electromagnetic waves with very low frequencies.

In [9] it has been shown that one insulating obstacle is uniquely determined by the associated backscatter data: The proof given in [9] is constructive and can be utilized for a numerical algorithm to be published elsewhere. A shortcoming of this approach, however, is that the method appears to break down if the inclusion has different physical properties (it can be extended to perfect conductors, though), or if more than one obstacle exists within the body.

Both of these limitations can be managed to some extent with an approach that goes back to work by Kusiak and Sylvester [22], who introduced in 2003 the concept

*Institut für Mathematik, Johannes Gutenberg-Universität Mainz, 55099 Mainz, Germany (hanke@math.uni-mainz.de).

†Institute of Mathematics, Helsinki University of Technology, FI-02015 HUT, Finland (nuutti.hyvonen@hut.fi). The work of N. Hyvönen was supported by the Academy of Finland (project 115013), the Finnish Cultural Foundation, the Finnish Foundation for Technology Promotion, and the Finnish Funding Agency for Technology and Innovation (project 40084/06).

‡Institut für Mathematik, Johannes Gutenberg-Universität Mainz, 55099 Mainz, Germany (reusswig@math.uni-mainz.de). The work of S. Reusswig was supported by the Deutsche Forschungsgemeinschaft (DFG) under grant HA 2121/6.

of *scattering supports* for the localization of admissible sources for a given scattered wave (in the regime of the Helmholtz equation). This idea has been carried over by the present authors to the Laplace equation in [7], to the inverse obstacle problem in impedance tomography with ‘traditional’ data in [8], and, by Haddar, Kusiak, and Sylvester [5], to the ‘usual’ backscattering problem for the Helmholtz equation.

In this paper, we apply the techniques from [7, 8] to the aforementioned backscattering problem in impedance tomography. To this end, we start by showing that the backscatter data can be interpreted as the boundary values of a potential that satisfies the Laplace equation with homogeneous Neumann data and a source term supported in the convex hull of the inclusion(s). In fact, we show that they are the boundary values of a *holomorphic* function. Under mild restrictions on the topological properties of the inclusions the domain of analyticity of this potential extends even up to the boundary of the inclusions. We can then use the algorithm described in [8] to numerically compute what we call the *convex backscattering support*, i.e., the smallest convex set that carries an electrostatic source for which the associated potential coincides with the backscatter data on the object boundary. As such, this set is guaranteed to be a subset of the convex hull of the true inclusion(s), and can thus be utilized to localize them. We mention that these results match well with the corresponding ones from [5] for the Helmholtz equation, although the methods from [5] do not appear to extend to our setting.

Numerical results indicate that our method provides very reasonable approximations of the inclusions in the absence of noise – even better ones than those in [8] for the traditional measurement setup with the boundary potential for one fixed input current as data. Being a severely ill-posed problem, though, the reconstructions deteriorate in the presence of measurement noise, but can still be used to localize the unknown inclusions for a moderate amount of noise.

In Section 2, we provide a rigorous specification of the particular version of the inverse obstacle problem that we are looking at and, in particular, review our notion of backscatter data. Then, in Sections 3 and 4 we prove that these data are the boundary values of a function that is holomorphic in the homogeneous part of the object, imposing only very mild restrictions on the topological properties of the inclusions. To this end, we first investigate the difference of two Neumann-to-Dirichlet operators that are familiar objects in the analysis of inverse obstacle problems in impedance tomography, and utilize a factorization of this difference operator similar to others that have already been used quite successfully in the context of the so-called *factorization methods*, see Brühl [1], Kress and Kühn [20], and Gebauer [4], for example. Subsequently, in Section 5, we briefly recall the definition of the convex source support from [7], and show how to apply the corresponding theory to localize the convex hull of the inclusions from the given backscatter data. Finally, some numerical reconstructions are presented in Section 6.

2. Problem setting. Let D be the open unit disk and assume that the conductivity $\sigma \in L^\infty(D)$ inside D satisfies the conditions

$$\sigma \geq c > 0 \quad \text{and} \quad \text{supp}(\sigma - 1) \text{ is a compact subset of } D,$$

which means, in particular, that $\sigma = 1$ near the boundary $T = \partial D$. Of course, the support of $\sigma - 1$ can be very complicated topologically. We therefore fix an open set Σ , which consists of finitely many simply connected domains Σ_j , $j = 1, \dots, m$, with $\overline{\Sigma}_i \cap \overline{\Sigma}_j = \emptyset$ for $i \neq j$, such that

$$\text{supp}(\sigma - 1) \subset \overline{\Sigma} \subset D.$$

For example, if σ is piecewise smooth, and the support of $\sigma - 1$ itself consists of m connected components, then Σ could be such that $\overline{\Sigma}$ becomes what has been called the *infinity support* of $\sigma - 1$ in [7, 22], i.e., the set of points that cannot be connected to infinity without intersecting the support of $\sigma - 1$. As another very simple example, we could choose Σ to be the interior of the convex hull of $\text{supp}(\sigma - 1)$. In fact, this latter situation will move into our focus for the numerical examples in the second part of this paper.

We consider the boundary value problem

$$\nabla \cdot (\sigma \nabla u) = 0 \quad \text{in } D, \quad \frac{\partial}{\partial \nu} u = f \quad \text{on } T, \quad (2.1)$$

where ν is the exterior unit normal of T . For any boundary current f in

$$H_{\diamond}^s(T) = \{g \in H^s(T) \mid \langle g, 1 \rangle = 0\}, \quad s \in \mathbb{R}, \quad (2.2)$$

problem (2.1) has a unique solution u in

$$\mathcal{H}_s := (H^{\min\{1, s+3/2\}}(D) \cap H_{\text{loc}}^1(D)) / \mathbb{C}, \quad (2.3)$$

where

$$H_{\text{loc}}^1(D) = \{v \in \mathcal{D}'(D) \mid v|_U \in H^1(U) \text{ for every open } U \text{ with } \overline{U} \subset D\};$$

see Theorem A.2 in the appendix. Here and in what follows, $\langle \cdot, \cdot \rangle : H^s(T) \times H^{-s}(T) \rightarrow \mathbb{C}$ denotes the dual evaluation between Sobolev spaces on T ; if there is no possibility for a mix-up we refrain from marking the spaces in brackets and use this same notation for the induced duality between $H_{\diamond}^s(T)$ and $H^{-s}(T)/\mathbb{C}$.

REMARK 1. The norm of a generic quotient distribution space H/\mathbb{C} is defined in the natural way:

$$\|v\|_{H/\mathbb{C}} = \inf_{c \in \mathbb{C}} \|v - c\|_H. \quad (2.4)$$

On the left-hand side of (2.4), v denotes an element of H/\mathbb{C} , i.e., an equivalence class, whereas on the right-hand side v stands for any particular representative of the class in question. Unless there is a possibility of confusion, we do not distinguish between quotient equivalent classes and elements spanning them. It is well-known that (2.4) defines a norm and H/\mathbb{C} inherits completeness from H . Note, in particular, that

$$c \|\nabla v\|_{L^2(D)} \leq \|v\|_{H^1(D)/\mathbb{C}} \leq C \|\nabla v\|_{L^2(D)}$$

for some $C \geq c > 0$ independent of $v \in H^1(D)/\mathbb{C}$ (cf. Lemma 2.5 of [13]). \square

REMARK 2. The definition of \mathcal{H}_s as a quotient space emphasizes the fact that the electromagnetic potential is unique up to the choice of the ground level, that is, up to an additive constant. For regular input currents, i.e., for $s \geq -1/2$, the solution space \mathcal{H}_s is just $H^1(D)/\mathbb{C}$; even if $s > -1/2$, one cannot ask for more regularity in the whole of D since σ is only assumed to be in $L^\infty(D)$. On the other hand, \mathcal{H}_s equals $(H^{s+3/2}(D) \cap H_{\text{loc}}^1(D)) / \mathbb{C}$ if $s < -1/2$: Although a distributional input current makes the corresponding potential irregular near the boundary T , the solution u of (2.1) will still possess enough ‘interior regularity’ to make the multiplication of ∇u by σ well defined in the support of $\sigma - 1$. \square

We define the Neumann-to-Dirichlet, or current-to-voltage, map Λ via

$$\Lambda : f \mapsto u|_T, \quad H_{\diamond}^s(T) \rightarrow H^{s+1}(T)/\mathbb{C}, \quad (2.5)$$

which is well defined and bounded for every $s \in \mathbb{R}$ according to Theorem A.3 in the appendix. In the same manner, we introduce the reference Neumann-to-Dirichlet map

$$\Lambda_0 : f \mapsto u_0|_T, \quad H_\diamond^s(T) \rightarrow H^{s+1}(T)/\mathbb{C},$$

where $u_0 \in H^{s+3/2}(D)/\mathbb{C}$ is the unique solution of (2.1) when σ is replaced by 1, cf. Lions and Magenes [23, Chapter 2, Remark 7.2], i.e.,

$$\Delta u_0 = 0 \quad \text{in } D, \quad \frac{\partial}{\partial \nu} u_0 = f \quad \text{on } T. \quad (2.6)$$

Since σ is identically 1 in some (interior) neighborhood of T , it follows from the regularity theory of elliptic partial differential equations that $u - u_0$ is smooth near the boundary T , and, in fact, that the difference boundary map

$$\Lambda - \Lambda_0 : H_\diamond^{-s}(T) \rightarrow H^s(T)/\mathbb{C} \quad (2.7)$$

is bounded for every $s \in \mathbb{R}$; see Theorem A.3 again.

Let us then consider a more specific local current pattern $f = \delta'_\theta \in H^{-3/2-\epsilon}(T)$, $\epsilon > 0$, which is defined by

$$\langle \delta'_\theta, v \rangle = - \frac{\partial v}{\partial \tau}(z_\theta) \quad \text{for every } v \in H^{3/2+\epsilon}(T), \quad (2.8)$$

where $z_\theta = (\cos \theta, \sin \theta)$ and τ is the arc length parameter of T . Since δ'_θ has zero mean, i.e., $\langle \delta'_\theta, 1 \rangle = 0$, and due to the continuity of the boundary operator (2.7), the quantity

$$b(z_\theta) = \langle (\Lambda - \Lambda_0)\delta'_\theta, \delta'_\theta \rangle \quad (2.9)$$

is well defined. The function $b : T \rightarrow \mathbb{R}$ is what we call the backscatter data; see [9] for an interpretation of b as data gathered by a single (small) pair of close electrodes moving along the boundary T . Note that $b(z_\theta)$ is defined by measurements made at the single point z_θ , and thus our data is truly local in nature.

3. Factorization of $\Lambda - \Lambda_0$. We choose Ω_j , $j = 1, \dots, m$, to be simply connected C^∞ -domains, such that $\overline{\Sigma}_j \subset \Omega_j$, $\overline{\Omega}_j \subset D$ and $\overline{\Omega}_i \cap \overline{\Omega}_j = \emptyset$ for $i \neq j$, and let Γ_j be the boundary of Ω_j . We set $\Omega = \cup \Omega_j$, and denote by $\Gamma = \cup \Gamma_j$ its boundary. Then we introduce the spaces

$$H^1(\Omega)/\mathbb{C}^m := (H^1(\Omega_1)/\mathbb{C}) \oplus \dots \oplus (H^1(\Omega_m)/\mathbb{C})$$

and

$$H^s(\Gamma)/\mathbb{C}^m := (H^s(\Gamma_1)/\mathbb{C}) \oplus \dots \oplus (H^s(\Gamma_m)/\mathbb{C}), \quad s \in \mathbb{R}.$$

The dual space of $H^s(\Gamma)/\mathbb{C}^m$ with respect to the dual pairing induced by the $L^2(\Gamma)$ inner product is

$$H_{\diamond}^{-s}(\Gamma) := H_{\diamond}^{-s}(\Gamma_1) \oplus \dots \oplus H_{\diamond}^{-s}(\Gamma_m), \quad (3.1)$$

where the component spaces are defined in accordance with (2.2).

Now, consider the boundary value problem

$$\Delta v = 0 \quad \text{in } D \setminus \overline{\Omega}, \quad \frac{\partial}{\partial \nu} v = f \quad \text{on } T, \quad \frac{\partial}{\partial \nu} v = 0 \quad \text{on } \Gamma, \quad (3.2)$$

where ν is the exterior unit normal of Γ . For any $f \in H_\diamond^s(T)$, problem (3.2) has a unique solution $v \in H^{s+3/2}(D \setminus \overline{\Omega})/\mathbb{C}$ (cf. [23, Chapter 2, Remark 7.2]), which is smooth near the inner boundary Γ due to the regularity theory for elliptic partial differential equations. In fact, the linear operator

$$R : f \mapsto v|_\Gamma, \quad H_\diamond^s(T) \rightarrow H^{1/2}(\Gamma)/\mathbb{C}^m, \quad (3.3)$$

is bounded for every $s \in \mathbb{R}$ (cf. Theorem A.3). Although the Dirichlet trace of v on Γ is indeed defined up to only one additive constant, here we interpret $v|_\Gamma$ as an element of $H^{1/2}(\Gamma)/\mathbb{C}^m$ by letting each component $v|_{\Gamma_j}$, $j = 1, \dots, m$, of $v|_\Gamma$ define an equivalence class in the corresponding component quotient space $H^{1/2}(\Gamma_j)/\mathbb{C}$; notice that — even with this interpretation — R is injective due to the principle of unique continuation. According to Brühl [1] (in full generality, as it is required here, the result can be found in [10]) the difference $\Lambda - \Lambda_0$ obeys the factorization

$$\Lambda - \Lambda_0 = R^* F R, \quad (3.4)$$

where $F : H^{1/2}(\Gamma)/\mathbb{C}^m \rightarrow H_\diamond^{-1/2}(\Gamma)$ is a bounded linear operator that coincides with its own dual.

To be more precise, F is defined with the help of the transmission problem

$$\begin{aligned} \nabla \cdot (\sigma \nabla h) &= 0 \quad \text{in } D \setminus \Gamma, & \frac{\partial}{\partial \nu} h &= 0 \quad \text{on } T, \\ h^+ - h^- &= \psi, & \frac{\partial}{\partial \nu} h^+ - \frac{\partial}{\partial \nu} h^- &= 0 \quad \text{on } \Gamma, \end{aligned} \quad (3.5)$$

where the superscripts $+$ and $-$ correspond to traces taken from within $D \setminus \overline{\Omega}$ and Ω , respectively. The problem (3.5) has a unique solution $h \in (H^1(\Omega)/\mathbb{C}^m) \oplus (H^1(D \setminus \overline{\Omega})/\mathbb{C})$ that depends continuously on the data $\psi \in H^{1/2}(\Gamma)/\mathbb{C}^m$ (cf., e.g., Kirsch [18, p. 262], or [10]). The operator F in the middle of the factorization (3.4) is given by

$$F : \psi \mapsto \frac{\partial}{\partial \nu} (h - h_0)|_\Gamma,$$

where h_0 is the solution of (3.5) when σ is replaced by 1. By virtue of Green's identity (applied to each subdomain Ω_j), $F\psi$ belongs to $H_\diamond^{-1/2}(\Gamma)$. Moreover, there exists a representative of the equivalence class $h - h_0$ that has continuous Dirichlet trace over every Γ_j and thus satisfies the Laplace equation in some neighborhood of Γ . In consequence, it follows from the regularity theory for elliptic partial differential equations that F can, in fact, be extended to a bounded map

$$F : H^s(\Gamma)/\mathbb{C}^m \rightarrow H_\diamond^{-s}(\Gamma) \quad (3.6)$$

for any $s \in \mathbb{R}$ (cf. Theorem A.3).

For our purposes it would be useful to have a factorization similar to (3.4) with R replaced by the linear operator

$$B : f \mapsto u_0|_\Gamma, \quad H_\diamond^s(T) \rightarrow H^{1/2}(\Gamma)/\mathbb{C}^m, \quad (3.7)$$

where u_0 is the unique solution of (2.6) and $u_0|_\Gamma$ is interpreted as an element of $H^{1/2}(\Gamma)/\mathbb{C}^m$ in the same sense as $v|_\Gamma$ in (3.3). Once again, we refer to Theorem A.3 for a proof that B is well defined and bounded. Such a factorization has indeed been

derived previously by Kress and Kühn [20] for a very similar problem. Here, we utilize the results from [1, 10] instead to establish this alternative factorization.

To this end, we introduce two auxiliary operators

$$\begin{aligned}\Lambda_1^{-1} : \psi &\mapsto \frac{\partial v_1}{\partial \nu} \Big|_{\Gamma}, & H^{1/2}(\Gamma)/\mathbb{C}^m &\rightarrow H_{\infty}^{-1/2}(\Gamma), \\ \Lambda_2 : \phi &\mapsto v_2|_{\Gamma}, & H_{\infty}^{-1/2}(\Gamma) &\rightarrow H^{1/2}(\Gamma)/\mathbb{C}^m.\end{aligned}\tag{3.8}$$

Here, $v_1 \in H^1(\Omega)/\mathbb{C}^m$ is the unique solution of the Dirichlet problem

$$\Delta v_1 = 0 \quad \text{in } \Omega, \quad v_1 = \psi \quad \text{on } \Gamma,\tag{3.9}$$

and $v_2 \in H^1(D \setminus \overline{\Omega})/\mathbb{C}$ is the unique solution of the Neumann problem

$$\Delta v_2 = 0 \quad \text{in } D \setminus \overline{\Omega}, \quad \frac{\partial}{\partial \nu} v_2 = 0 \quad \text{on } T, \quad \frac{\partial}{\partial \nu} v_2 = \phi \quad \text{on } \Gamma,\tag{3.10}$$

whose Dirichlet trace on Γ is interpreted as an element of $H^{1/2}(\Gamma)/\mathbb{C}^m$. Take note that both Λ_1^{-1} and Λ_2 remain bounded operators, if the Sobolev smoothness indices $1/2$ and $-1/2$ in (3.8) are replaced by s and $s-1$, respectively, for any $s \in \mathbb{R}$; see [23, Chapter 2, Remark 7.2] and the trace theorems [23, Chapter 1, Theorem 9.4] and [23, Chapter 2, Theorems 6.5 and 7.3], together with the related remarks. The following lemma shows how the operator R of (3.3) can be rewritten with the help of B , Λ_1^{-1} and Λ_2 .

LEMMA 3.1. *The operator R obeys the factorization*

$$R = (I - \Lambda_2 \Lambda_1^{-1})B$$

where I is the identity operator.

Proof. Let $u_0 \in H^{s+3/2}(D)/\mathbb{C}$ be the solution of (2.6), and let $v_2 \in H^1(D \setminus \overline{\Omega})/\mathbb{C}$ be the solution of (3.10) for $\phi = (\partial u_0 / \partial \nu)|_{\Gamma}$, which is a smooth and mean-free function on each Γ_j (cf. Lemma A.1 in the appendix). Since $u_0|_{\Omega}$ satisfies (3.9) for $\psi = u_0|_{\Gamma}$, it follows that $(\partial u_0 / \partial \nu)|_{\Gamma} = \Lambda_1^{-1} B f$, and hence

$$(I - \Lambda_2 \Lambda_1^{-1})B f = (u_0 - v_2)|_{\Gamma}.$$

Since the difference $u_0|_{D \setminus \overline{\Omega}} - v_2$ satisfies (3.2), the proof is complete. \square

Making use of Lemma 3.1 in (3.4), we obtain the factorization sought after:

COROLLARY 3.2. *The operator $\Lambda - \Lambda_0$ can be factored as*

$$\Lambda - \Lambda_0 = B^* G B,\tag{3.11}$$

where $G : H^{1/2}(\Gamma)/\mathbb{C}^m \rightarrow H_{\infty}^{-1/2}(\Gamma)$ is a bounded linear operator, which coincides with its dual operator. Moreover, G can be extended to a continuous operator from $H^s(\Gamma)/\mathbb{C}^m$ to $H_{\infty}^{-s}(\Gamma)$ for any $s \in \mathbb{R}$.

Proof. The first part of the claim follows immediately from (3.4) and Lemma 3.1. The second part is a consequence of the boundedness of the map (3.6) together with the fact that $(I - \Lambda_2 \Lambda_1^{-1})$ maps $H^s(\Gamma)/\mathbb{C}^m$ continuously to itself for any $s < 1/2$. \square

REMARK 3. In [1, 10] the factorization (3.4) has been established when $\Lambda - \Lambda_0$ is considered as an operator on $H_{\infty}^{-1/2}(T)$, but the result extends, e.g., by continuity, to the more general case considered in this work. Also, although it has been assumed in [1, 10] that Γ is a (smooth) boundary of an inhomogeneity, the factorization (3.4)

holds true for any (finite set of) smooth injective curves Γ_j separating the inclusions and the outer boundary T (cf. [15, Theorem 3.1]). Finally, as in [1, 10] we have treated F as an operator from $H^{1/2}(\Gamma)/\mathbb{C}^m$ to $H_\infty^{-1/2}(\Gamma)$, but it follows easily that F is, actually, well defined and bounded on the whole of $H^{1/2}(\Gamma)$ and maps functions that are constant on each component Γ_j of Γ to zero. To see the latter, take note that for such piecewise constant ψ the solution h of (3.5) is constant on each subdomain Ω_j , and on $D \setminus \overline{\Omega}$. Hence, F , and G , may indeed, be treated as bounded operators between $H^{1/2}(\Gamma)$ and $H^{-1/2}(\Gamma)$, or $H^s(\Gamma)$ and $H^{-s}(\Gamma)$ for any $s \in \mathbb{R}$; this interpretation will be useful when proving Theorem 4.2 below. \square

4. Analyticity of the backscatter data. In this section, we will use the factorization (3.11) to show that the backscatter data can be interpreted as the boundary value of a function that is (complex) analytic in $D \setminus \overline{\Sigma}$, where Σ has been fixed in Section 2. To this end, let Ω and Γ be as in the previous section, and note that for smooth enough f the function Bf — or more precisely, one representative of the equivalence class — can be written as

$$Bf(x) = \int_T N(x, z) f(z) ds(z), \quad x \in \Gamma, \quad (4.1)$$

where N is the Neumann function for the Laplacian in D , i.e.,

$$N(x, z) = \begin{cases} -\frac{1}{2\pi} \left(\log|x-z| + \log \left| \frac{x}{|x|} - |x|z \right| \right), & x \neq 0, \\ -\frac{1}{2\pi} \log|z|, & x = 0. \end{cases} \quad (4.2)$$

Using the density of, say, $C_\infty^\infty(T)$ in $H_\infty^{-3/2-\epsilon}(T)$ and the continuous dependence of the solution of (2.6) on the Neumann data (cf. [23, Chapter 2, Remark 7.2]), it follows that

$$B\delta'_\theta(x) = -\frac{\partial}{\partial z\tau} N(x, z)|_{z=z_\theta} = -\frac{1}{\pi} \frac{x \cdot z_\theta^\perp}{|x - z_\theta|^2}, \quad x \in \Gamma,$$

where $z_\theta^\perp = (-\sin \theta, \cos \theta)$.

By introducing the complex numbers $\xi = \xi(x) = x_1 + ix_2$ and $\zeta = e^{i\theta}$, and identifying D and Ω where necessary with the corresponding subsets of the complex plane, we obtain the representation

$$B\delta'_\theta(x) = \frac{1}{2\pi i} \frac{\bar{\xi}\zeta - \xi\bar{\zeta}}{(\xi - \zeta)(\bar{\xi} - \bar{\zeta})} = \frac{i}{2\pi} \frac{\bar{\xi}\zeta^2 - \xi}{(\zeta - \xi)(\bar{\xi}\zeta - 1)} =: g(x, \zeta), \quad x \in \Gamma, \quad (4.3)$$

which obviously extends as continuous function to $\Gamma \times (\overline{D} \setminus \overline{\Omega})$. The extended g — still denoted by the same symbol — is complex differentiable with respect to ζ , and also $\partial_\zeta g(x, \zeta)$ is a continuous function of $(x, \zeta) \in \Gamma \times (\overline{D} \setminus \overline{\Omega})$. The following lemma demonstrates that $[Gg(\cdot, \zeta)](x)$ has the same properties as $g(x, \zeta)$; here G is the operator that was introduced in Corollary 3.2.

LEMMA 4.1. *The function $[Gg(\cdot, \zeta)](x)$, $(x, \zeta) \in \Gamma \times (D \setminus \overline{\Omega})$, is complex differentiable with respect to ζ . Moreover, both $[Gg(\cdot, \zeta)](x)$ and $\partial_\zeta [Gg(\cdot, \zeta)](x)$ are continuous in $\Gamma \times (\overline{D} \setminus \overline{\Omega})$.*

Proof. To begin with, note that G maps $C(\Gamma)$ continuously to $C(\Gamma)$ due to Corollary 3.2 and the Sobolev embedding theorems; see [3, p.100] and [23, Chapter 1, Section 7.3]. Recall that the norm of $C(\Gamma)$ is defined by

$$\|\psi\|_{C(\Gamma)} = \max_{x \in \Gamma} |\psi(x)|$$

for $\psi \in C(\Gamma)$.

Let $\{x_j\} \subset \Gamma \subset \mathbb{R}^2$ and $\{\zeta_j\} \subset \overline{D} \setminus \overline{\Omega} \subset \mathbb{C}$ be two sequences that converge to fixed but arbitrary points $x \in \Gamma$ and $\zeta \in \overline{D} \setminus \overline{\Omega}$, respectively. With the help of the boundedness of $G : C(\Gamma) \rightarrow C(\Gamma)$, we obtain

$$\begin{aligned} & \left| [Gg(\cdot, \zeta)](x) - [Gg(\cdot, \zeta_j)](x_j) \right| \\ & \leq \left| [Gg(\cdot, \zeta)](x) - [Gg(\cdot, \zeta)](x_j) \right| + \left| [Gg(\cdot, \zeta)](x_j) - [Gg(\cdot, \zeta_j)](x_j) \right| \quad (4.4) \\ & \leq \left| [Gg(\cdot, \zeta)](x) - [Gg(\cdot, \zeta)](x_j) \right| + C \|g(\cdot, \zeta) - g(\cdot, \zeta_j)\|_{C(\Gamma)}. \end{aligned}$$

Since $g(z, \zeta)$ is a continuous function of $z \in \Gamma$, so is $[Gg(\cdot, \zeta)](z)$, and thus the first term on the right-hand side of (4.4) converges to zero as j goes to infinity. On the other hand, it follows immediately from the representation (4.3) and the compactness of Γ that $g(\cdot, \zeta_j)$ converges to $g(\cdot, \zeta)$ in the topology of $C(\Gamma)$. Hence, we have shown that $[Gg(\cdot, \zeta)](x)$ is continuous as function of $(x, \zeta) \in \Gamma \times (\overline{D} \setminus \overline{\Omega})$.

For a fixed $\zeta \in D \setminus \overline{\Omega}$, it follows again from (4.3) and the compactness of Γ that

$$\frac{g(\cdot, \zeta + \delta) - g(\cdot, \zeta)}{\delta} \rightarrow \partial_\zeta g(\cdot, \zeta) \quad \text{as } \delta \rightarrow 0, \delta \neq 0,$$

in the topology of $C(\Gamma)$. As a consequence, for any $x \in \Gamma$,

$$\frac{1}{\delta} \left([Gg(\cdot, \zeta + \delta)](x) - [Gg(\cdot, \zeta)](x) \right) \rightarrow [G\partial_\zeta g(\cdot, \zeta)](x) \quad \text{as } \delta \rightarrow 0, \quad (4.5)$$

due to the linearity and continuity of $G : C(\Gamma) \rightarrow C(\Gamma)$; actually, the limit (4.5) is uniform with respect to $x \in \Gamma$. We conclude that $[Gg(\cdot, \zeta)](x)$ is complex differentiable with respect to $\zeta \in D \setminus \overline{\Omega}$. Finally, the continuity of $\partial_\zeta [Gg(\cdot, \zeta)](x) = [G(\partial_\zeta g(\cdot, \zeta))](x)$ in $\Gamma \times (\overline{D} \setminus \overline{\Omega})$ follows from the same line of reasoning as that of $[Gg(\cdot, \zeta)](x)$. \square

Since $g(x, \zeta)$ is real if $\zeta \in T$, the factorization (3.11) and a slight abuse of notation provide us with the formula

$$b(\zeta) = \int_\Gamma [Gg(\cdot, \zeta)](x) g(x, \zeta) \, ds(x), \quad \zeta \in T, \quad (4.6)$$

for the backscatter data b from (2.9). Apparently, the right-hand side of (4.6) extends to a well defined function of ζ in the whole of $\overline{D} \setminus \overline{\Omega}$. Our aim is to show that this extension is holomorphic.

THEOREM 4.2. *The backscatter data b of (2.9) extends as a holomorphic function to $D \setminus \overline{\Sigma}$, with Σ as defined in Section 2.*

Proof. According to Lemma 4.1 and the material preceding it, the function $[Gg(\cdot, \zeta)](x)g(x, \zeta)$, $(x, \zeta) \in \Gamma \times (\overline{D} \setminus \overline{\Omega})$, is continuous, holomorphic in ζ , and the corresponding complex derivative with respect to ζ is also continuous on $\Gamma \times (\overline{D} \setminus \overline{\Omega})$. As a consequence, it follows from an obvious variant of [25, Proposition 27] that (4.6) gives a holomorphic extension of the backscatter data to $D \setminus \overline{\Omega}$.

Next we will show that the extension of the backscatter data provided by (4.6) is independent of the particular choice of Ω (not taking into account the domain of definition, of course). To this end, let b_1 and b_2 be the holomorphic extensions of the backscatter data given by (4.6) for two different auxiliary sets $\Omega^{(1)}$ and $\Omega^{(2)}$, respectively. We choose a third C^∞ -set $\Omega^{(3)}$ fulfilling the requirements of Section 3, such that $\Omega^{(3)} \subset \Omega^{(k)}$, $k = 1, 2$, and we denote the corresponding holomorphic extension of the backscatter to $D \setminus \overline{\Omega^{(3)}}$ by b_3 . Since all three extensions have the same boundary value on T , it follows from the principle of unique continuation that

$$b_1 = b_3|_{D \setminus \overline{\Omega^{(1)}}} \quad \text{and} \quad b_2 = b_3|_{D \setminus \overline{\Omega^{(2)}}},$$

and, in particular, b_1 and b_2 coincide in the intersection of their domains of definition, i.e., in $D \setminus (\overline{\Omega^{(1)}} \cup \overline{\Omega^{(2)}})$ — even if it is not connected.

Finally, for any $\zeta_0 \in D \setminus \overline{\Sigma}$ we can choose a C^∞ -set Ω as prescribed in Section 3 such that $\zeta_0 \notin \Omega$, and use (4.6) to continue the backscatter data holomorphically to a neighborhood of ζ_0 . Thus, we conclude that the backscatter data extends as a univalent holomorphic function to the whole of $D \setminus \overline{\Sigma}$. \square

Let us then (re)identify the complex plane with \mathbb{R}^2 and write the (extended) backscatter data as a complex-valued function of $z \in \mathbb{R}^2$:

$$b(z) = u_b(z) + iv_b(z), \quad z \in D \setminus \overline{\Sigma}, \quad (4.7)$$

where u_b and v_b are real-valued. It follows from Theorem 4.2 that u_b is the solution of a certain Cauchy problem for the Laplacian in $D \setminus \overline{\Sigma}$.

COROLLARY 4.3. *The function u_b of (4.7) satisfies the Cauchy problem*

$$\Delta u_b = 0 \quad \text{in } D \setminus \overline{\Sigma}, \quad u_b = b \quad \text{on } T, \quad \frac{\partial}{\partial \nu} u_b = 0 \quad \text{on } T. \quad (4.8)$$

Proof. Since u_b is the real part of a holomorphic function, it is harmonic in its domain of definition $D \setminus \overline{\Sigma}$. Moreover, as $b|_T$ is real-valued, u_b and b coincide on T . Finally, because v_b — and, in particular, its tangential derivative — vanishes on T , it follows from the Cauchy-Riemann equations that u_b has vanishing normal derivative on T . Note that the Cauchy-Riemann equations may be used on T since b extends by reflection to a holomorphic function in some neighborhood of T , cf., e.g., Henrici [11]. \square

REMARK 4. It has been shown in [9, Corollary 3.4] that Theorem 4.2 and Corollary 4.3 are also valid for a simply connected insulating cavity within D , which would correspond to the degenerate situation where $\sigma = 0$ inside the inhomogeneity. Alternatively, one can treat insulating obstacles with the techniques of the previous sections by introducing homogeneous boundary conditions at the corresponding inclusions, to show that Theorem 4.2 and its corollary also apply if some obstacles are insulating while others are penetrable. In any case, it follows that the numerical algorithm to be presented below, applies to penetrable obstacles (with $\sigma \geq c > 0$) and insulating inclusions alike. \square

5. Convex backscattering support. Our aim is to show that the algorithm introduced in [8] can be applied to backscatter data to reconstruct an approximation of the convex hull of the inhomogeneities given by $\text{supp}(\sigma - 1)$. This set will be called the *convex backscattering support*, see Definition 5.1 below, in analogy to the corresponding definition in [5] within the context of acoustic scattering. We emphasize, however, that the mathematical techniques used here are different from those in [5].

In what follows, $b : T \rightarrow \mathbb{R}$ denotes again the given backscatter data of (2.9), Σ of Section 2 will be fixed to be the interior of the convex hull of $\text{supp}(\sigma - 1)$, and u_b is the solution of the Cauchy problem (4.8) in $D \setminus \overline{\Sigma}$. On occasion, we interpret $b = u_b|_T$ as an element of $L^2(T)/\mathbb{C}$.

We begin by considering the Poisson problem

$$\Delta w = F \quad \text{in } D, \quad \frac{\partial}{\partial \nu} w = 0 \quad \text{on } T, \quad (5.1)$$

which has a unique solution $w \in \bigcup_{m \in \mathbb{Z}} H^m(D)/\mathbb{C}$ for any distributional source F in

$$\mathcal{E}'_\diamond(D) = \{v \in \mathcal{E}'(D) \mid \langle v, 1 \rangle = 0\},$$

where $\langle \cdot, \cdot \rangle : \mathcal{E}'(D) \times C^\infty(D) \rightarrow \mathbb{C}$ denotes the dual evaluation between compactly supported distributions and smooth functions in D ; see [7, Section 2]. Since the solution w is smooth near the boundary T , the linear measurement operator

$$L : F \mapsto w|_T, \quad \mathcal{E}'_\diamond(D) \rightarrow L^2(T)/\mathbb{C},$$

is well defined.

DEFINITION 5.1. *Denote by $\text{supp}_c F$ the convex hull of the support $\text{supp} F$ of $F \in \mathcal{E}'_\diamond(D)$. Then the convex backscattering support $\mathcal{B}b$ is defined to be*

$$\mathcal{B}b = \bigcap_{LF=b} \text{supp}_c F.$$

The convex backscattering support $\mathcal{B}b$ is, in essence, the convex source support, as defined in [7, Definition 4.1], corresponding to the boundary data b . Theorem 5.2 below elucidates the significance of this definition, for it inherits useful properties from the convex source support. In what follows, we will denote the open ϵ -neighborhood and the convex hull of a set $\Omega \subset \mathbb{R}^2$ by $N_\epsilon(\Omega)$ and $\text{ch } \Omega$, respectively.

THEOREM 5.2. *The convex backscattering support $\mathcal{B}b$ is a subset of the convex hull $\overline{\Sigma}$ of the inhomogeneity $\text{supp}(\sigma - 1)$. Moreover, $\mathcal{B}b = \emptyset$, if and only if b is a constant, i.e., the zero element of $L^2(T)/\mathbb{C}$.*

Proof. We fix $\epsilon > 0$ such that $\overline{N_\epsilon(\Sigma)} \subset D$ and consider the $L^2(D)$ -function

$$w_\epsilon = \begin{cases} u_b & \text{in } D \setminus N_\epsilon(\Sigma), \\ 0 & \text{otherwise.} \end{cases}$$

According to Corollary 4.3, the source $F_\epsilon = \Delta w_\epsilon \in \mathcal{E}'_\diamond(D) \cap H^{-2}(D)$ is supported in $\overline{N_\epsilon(\Sigma)}$ and, moreover,

$$LF_\epsilon = w_\epsilon|_T = u_b|_T = b.$$

Since ϵ was chosen arbitrarily, we deduce that

$$\mathcal{B}b \subset \bigcap_{\epsilon > 0} \text{ch } \overline{N_\epsilon(\Sigma)} = \bigcap_{\epsilon > 0} \overline{N_\epsilon(\Sigma)} = \overline{\Sigma}.$$

This proves the first part of the assertion. The second part follows immediately from the properties of the convex source support established in [7, Theorem 4.1]. \square

From a practical point of view, the most important property of the convex backscattering support is that it can be approximated — or even defined — in a

constructive manner; see [8, Sections 3 and 4]. To this end, interpret b as a function of the polar angle and denote its Fourier coefficients by

$$\beta_j = \frac{1}{2\pi} \int_{-\pi}^{\pi} b(\theta) e^{-ij\theta} d\theta, \quad j \in \mathbb{Z}.$$

Moreover, define the auxiliary (extended) backscatter data as

$$b_\rho(\theta) = \sum_{j \in \mathbb{Z}} \frac{\beta_j}{\rho^{|j|}} e^{ij\theta}, \quad \theta \in [-\pi, \pi), \quad (5.2)$$

for $\rho \geq 1$ (cf. [8, Lemma 3.1]).

Let $B \subset \mathbb{R}^2$ be an arbitrary closed disk and B_ρ be an open disk of large enough radius $\rho > 0$ centered at the origin, such that $B_\rho \supset B$. There exists a Möbius transformation Φ that maps \overline{B}_ρ onto \overline{D} , and B onto some disk \overline{B}_R around the origin. The radius $R = R(B, \rho)$ of \overline{B}_R is uniquely determined by B and ρ . We denote the angular map corresponding to $\Phi|_{\partial B_\rho}$ by

$$\varphi: \theta \mapsto \arg \Phi(\rho e^{i\theta}), \quad [-\pi, \pi) \rightarrow [-\pi, \pi),$$

and the Fourier coefficients of $b_\rho \circ \varphi^{-1}$ by $\{\beta_j(\Phi)\}$, i.e.,

$$\beta_j(\Phi) = \frac{1}{2\pi} \int_{-\pi}^{\pi} b_\rho(\theta) e^{-ij\varphi(\theta)} \varphi'(\theta) d\theta, \quad j \in \mathbb{Z}. \quad (5.3)$$

With the help of these definitions, we have the following characterization, cf. [8, Corollary 3.3]: The convex backscattering support $\mathcal{B}b$ is a subset of B , if and only if

$$\sum_{j \in \mathbb{Z}} \frac{|\beta_j(\Phi)|^2}{(R + \epsilon)^{2|j|}} < \infty \quad (5.4)$$

for $R = R(B, \rho)$ and every $\epsilon > 0$.

The inequality (5.4) provides a means to test whether $\mathcal{B}b \subset B$ for any closed disk $B \subset \mathbb{R}^2$. Since the closed and convex set $\mathcal{B}b \subset \mathbb{R}^2$ is uniquely determined by all closed disks enclosing it, (5.4) can be used to formulate an efficient numerical algorithm for reconstructing the convex backscattering support.

6. Numerical reconstructions. In this section, we give a short description of the algorithm presented in detail in [8]; as stated in Section 5, this algorithm yields the convex backscattering support when used with backscatter data as input. Later on, we present some numerical reconstructions obtained in this way. In all of our numerical examples, the conductivity is constant in the connected components of the inhomogeneity $\text{supp}(\sigma - 1)$.

The algorithm checks for a number of (well chosen) disks whether they contain the convex backscattering support for given backscatter data or not. Subsequently, all those disks which do so are intersected to arrive at a reconstruction of the convex backscattering support.

Accordingly, the crucial part in terms of the algorithm's performance is a prudent choice of the disks to be examined as well as an effective criterion to determine whether a disk contains the convex backscattering support. We meet these demands by fixing $\rho > 1$ and considering Möbius transformations of the following type:

$$\Phi_\zeta(z) = \rho \frac{z - \zeta}{\rho^2 - \overline{\zeta}z}, \quad (6.1)$$

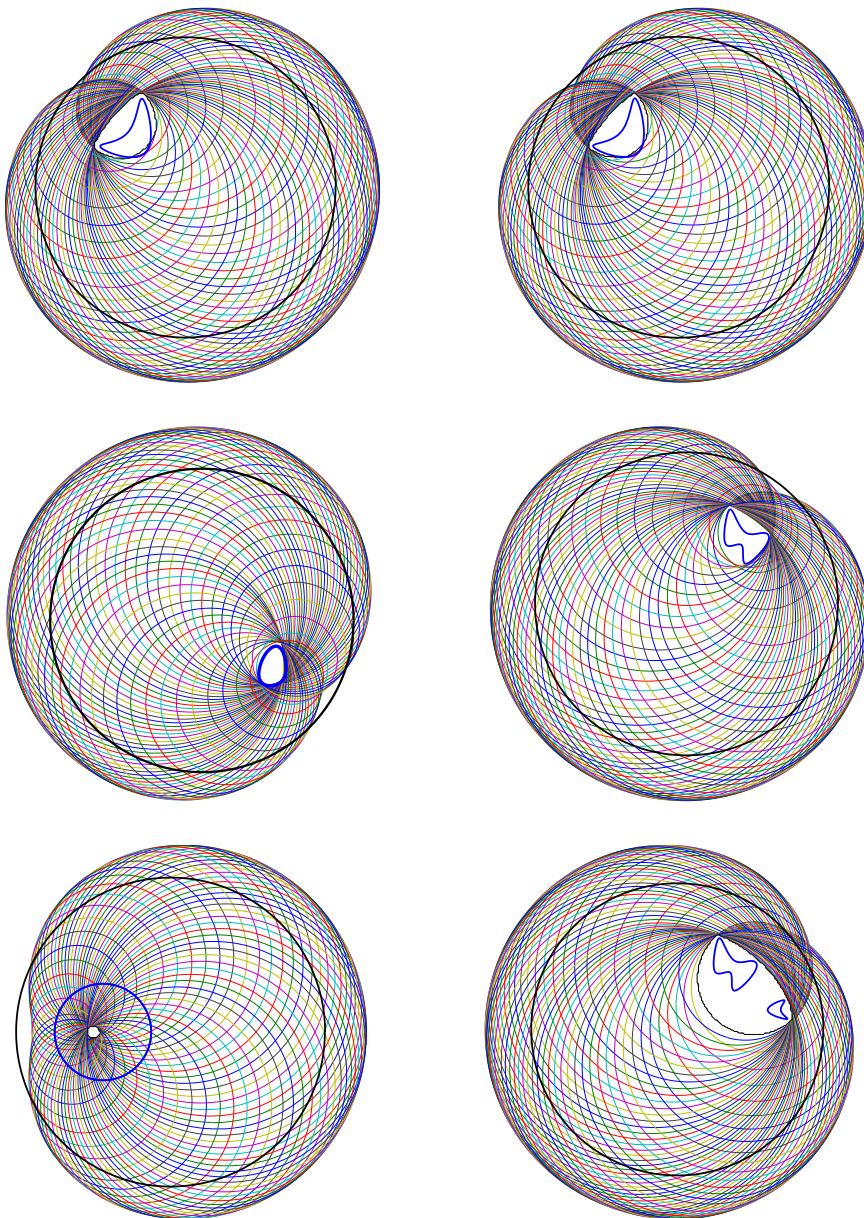


FIG. 6.1. Reconstructions of convex backscattering supports for insulating inclusions (left column) and conducting obstacles (right column; the conductivity within these obstacles is $\sigma = 0.5$, except for the small kite in the bottom row with conductivity $\sigma = 2$)

which map \overline{B}_ρ onto \overline{D} . Under Φ_ζ , the preimage of any disk \overline{B}_R with $0 < R < 1$ is a closed disk $\Phi_\zeta^{-1}(\overline{B}_R)$ containing the parameter point $\zeta \in B_\rho$, see [11]. As R varies, the corresponding disks $\Phi_\zeta^{-1}(\overline{B}_R)$ are nested. Our algorithm determines for any such Φ_ζ the smallest R_ζ for which the series in (5.4) converges. The convex backscattering support is then a subset of $B = \Phi_\zeta^{-1}(\overline{B}_{R_\zeta})$ but not of $\Phi_\zeta^{-1}(\overline{B}_R)$ for any $R < R_\zeta$, cf. [7,

Corollary 5.4].

As Φ_ζ in (6.1) is uniquely determined by ζ (for ρ fixed), we choose a grid Z of points $\zeta \in B_\rho$ and compute for each of these the minimal R_ζ . Finally, we approximate

$$\mathcal{B}b \approx \bigcap_{\zeta \in Z} \Phi_\zeta^{-1}(\overline{B}_{R_\zeta}). \quad (6.2)$$

Our experience shows that points ζ close to the origin scarcely contribute to the overall intersection in (6.2). Hence, we choose Z to be a set of M equidistant points on a concentric circle with radius $\rho_0 < \rho$. In terms of the stability of the algorithm, the parameters ρ and ρ_0 should be linked; see [8] for details. The setting of ρ in turn results from a trade-off between the quality of the approximation in (6.2) and the stability of the algorithm. That is to say, on the one hand, we approximate the convex set $\mathcal{B}b$ by intersecting subdisks of B_ρ . In this respect, if ρ is large, the approximation (6.2) improves as we can take more and larger disks into account. On the other hand, using (5.2) to extend the backscatter data to the boundary of a larger disk B_ρ results in a loss of information as subtleties in the data are levelled. According to our observations in [8], $\rho = 1.4$ and with it $\rho_0 = 0.7$ is a feasible choice.

To find the smallest R for which the series in (5.4) converges, we exploit the following observation: With increasing frequency, the Fourier coefficients $\{\beta_j(\Phi_\zeta)\}$ in (5.3) typically show exponential decay. Therefore, we estimate the decay rate of $\log |\beta_j(\Phi_\zeta)|$ by linear regression, i.e.,

$$\log |\beta_j(\Phi_\zeta)| \approx m|j| + c. \quad (6.3)$$

We now assume that the series in (5.4) converges whenever $R > e^m$, and hence let $R_\zeta = e^m$.

For our numerical experiments, we use a boundary element code to compute the relative boundary potential $(\Lambda - \Lambda_0)\delta'_\theta$ for $N = 768$ equidistant locations z_θ of the current dipole (cf. [9, Example 2.2]). From these, we collect the backscatter data (2.9) at the very same 768 grid points. To solve the inverse problem, we compute the ‘extended’ backscatter data b_ρ using (5.2), and the corresponding Fourier coefficients $\{\beta_j(\Phi_\zeta)\}$ of (5.3) for $M = 64$ equispaced parameters $\zeta \in \partial B_{\rho_0}$.

An important issue in terms of the stability of the algorithm is to decide which Fourier coefficients are reliable enough to be used in (6.3). The number of authentic coefficients does not only depend on the level of noise inherent in the data but also on the individual decay rate of the sequence (5.3) for each ζ . If there is only ‘numerical noise’, we choose the truncation index adaptively by cutting away all those frequencies which satisfy

$$|\beta_k(\Phi_\zeta)| < 2 \cdot 10^4 \min_j |\beta_j(\Phi_\zeta)|.$$

In the presence of (uniformly distributed) random noise of 1%, added on top of the data, we have found that only the first five Fourier coefficients contain reliable information and therefore use only those for the corresponding reconstructions.

Figure 6.1 presents different examples of reconstructions obtained in this manner from exact data. The pictures show as solid lines the unit circle (black) and the respective inclusion(s) (blue). Furthermore, the multicolored circles depict the boundaries of the 64 disks in (6.2) so that the white area displays their intersection.

In the first line of Figure 6.1, the convex hull of the inclusions and the computed convex backscattering supports almost coincide. The kite-shaped inclusion on the

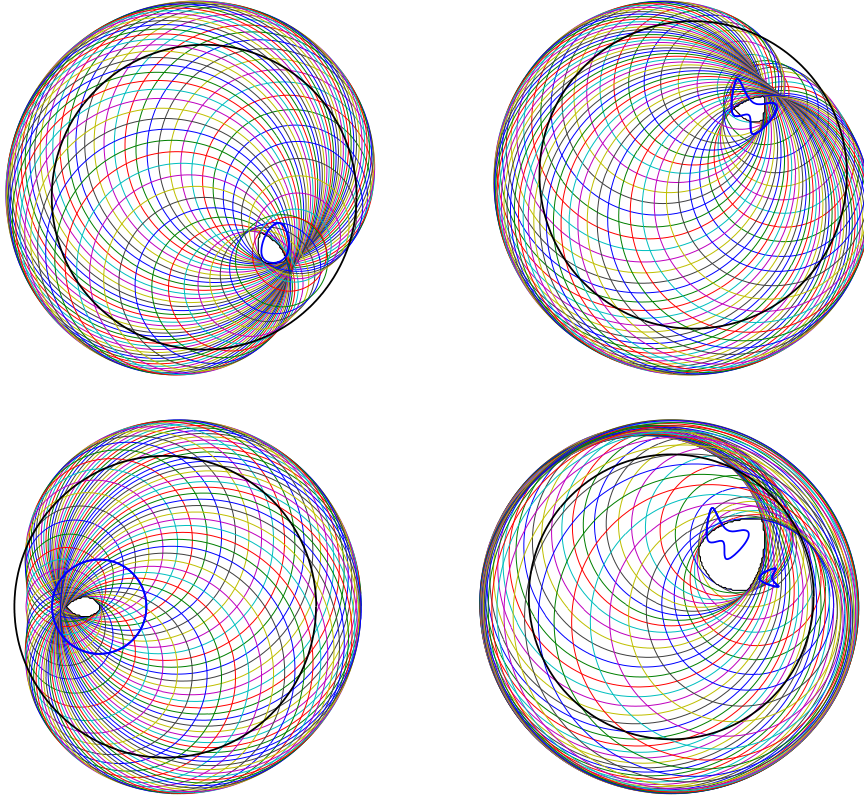


FIG. 6.2. Reconstructions of convex backscattering supports with 1% noise. The conductivities of the inclusions are as in the last two lines of Figure 6.1

left-hand side in the first line is insulating whereas the conductivity of the kite on the right is $\sigma = 0.5$. The reconstructions for the two cases are of comparable quality. We investigated the kite with conductivity $\sigma = 0.5$ before in [8], using there Dirichlet data corresponding to certain trigonometric input currents instead of backscatter data. The reconstructed inclusions obtained in [8] were generally smaller and less accurate than the reconstructions from backscatter data.

The two reconstructions in the middle row of Figure 6.1 also account for the accuracy of the convex backscattering support: The oval ($\sigma = 0$) on the left is almost exactly reconstructed. Likewise, the convex hull of the hourglass-shaped inclusion with $\sigma = 0.5$ is properly detected by the algorithm.

The left picture in the bottom line shows the case where the (insulating) inclusion is a disk. For this problem, the backscatter data can be continued analytically up to a single point in the interior of this disk, cf. [9, Corollary 3.4], and hence, the true convex backscattering support consists of only this one point. Again, this is properly reproduced by the algorithm.

As yet another example, in the bottom right image of Figure 6.1 we consider an instance with two inclusions of different conductivities, namely $\sigma = 0.5$ for the hourglass-shaped obstacle and $\sigma = 2$ for the small kite. As expected, the algorithm determines a convex set that contains both inclusions, not quite the convex hull,

though. Apparently, the difference in the conductivities of the two inclusions has no substantial effect on this reconstruction. This case shows how the choice of the parameter ρ affects the quality of the reconstruction: To improve the reconstruction we would need to enlarge ρ to include circles with small curvature in the ‘shadow region’ in the overall intersection (6.2). In fact, the reconstruction does improve, e.g., if $\rho = 2$; however, some of the other examples do not perform well with this larger value of ρ because of the increasing instabilities. We therefore stick to the well-trying parameter $\rho = 1.4$ also for this example.

In a second series of examples, we add 1% noise to the above considered data sets, and use only the first five Fourier coefficients for estimating the decay rate in (6.3). Figures 6.2 and 6.3 show the corresponding results. In the four examples of Figure 6.2 there is a distinct intersection of all 64 disks: The white area provides reliable information on the location of the inclusions whereas their shapes are no longer discernible.

As the intersection of the test disks is hardly distinguishable for the kite-shaped inclusions, cf. Figure 6.3, we present an alternative visualization of the respective intersection in the pictures on the right, where the intersection of the disks is highlighted in red. The first line corresponds to the insulating kite while the one in the second line has conductivity $\sigma = 0.5$. Again, the reconstructions indicate the location of the inclusion but carry no distinct information about its shape or size.

We have encountered reconstructions of similar quality for a series of examples with the same noise level. It is even possible to increase the noise level up to 5% and still be able to localize the inclusion at those points where most of the disks intersect. However, the intersection of *all* the disks is most often empty in this case, making it difficult to produce an approximation of the convex backscattering support by some general procedure.

7. Concluding remarks. We have shown that the backscatter data of impedance tomography can be interpreted as boundary values of a function of a complex variable that is holomorphic in $D \setminus \bar{\Sigma}$, where $\bar{\Sigma}$ coincides with the support of $\sigma - 1$ (together with the holes in it) under mild assumptions on the conductivity σ . For very rough conductivities, Σ can be chosen to consist of finitely many simply connected domains, such that $\bar{\Sigma}$ encloses the support of $\sigma - 1$. In particular, our results apply to the case that the closure of Σ is the convex hull of $\text{supp}(\sigma - 1)$. Assuming that the backscatter data is not constant, we can thus use the results from [7, 8] to numerically construct a nonempty convex set which we call the convex backscattering support, and which is always contained within the convex hull of $\text{supp}(\sigma - 1)$.

Our results have been formulated for the case that the object of interest is a disk. However, backscatter data are well-defined whenever the boundary of the domain is C^2 . We believe that our results can be extended to the case of more general simply connected two-dimensional objects with the help of the Riemann mapping theorem. This idea will be investigated in some future work.

Appendix. The purpose of this appendix is to show that problem (2.1) is uniquely solvable and to prove that the linear operators in (2.5), (2.7), (3.3), (3.6), and (3.7) are bounded. We begin with a lemma related to the interior regularity of certain potentials.

LEMMA A.1. *Let $U, U_0 \subset \mathbb{R}^2$ be two bounded C^∞ -domains such that $\bar{U} \subset U_0$. Assume that $v \in H^s(U_0)/\mathbb{C}$, $s \in \mathbb{R}$, is harmonic. Then,*

$$\|v\|_{H^r(U)/\mathbb{C}} \leq C(r)\|v\|_{H^s(U_0)/\mathbb{C}},$$

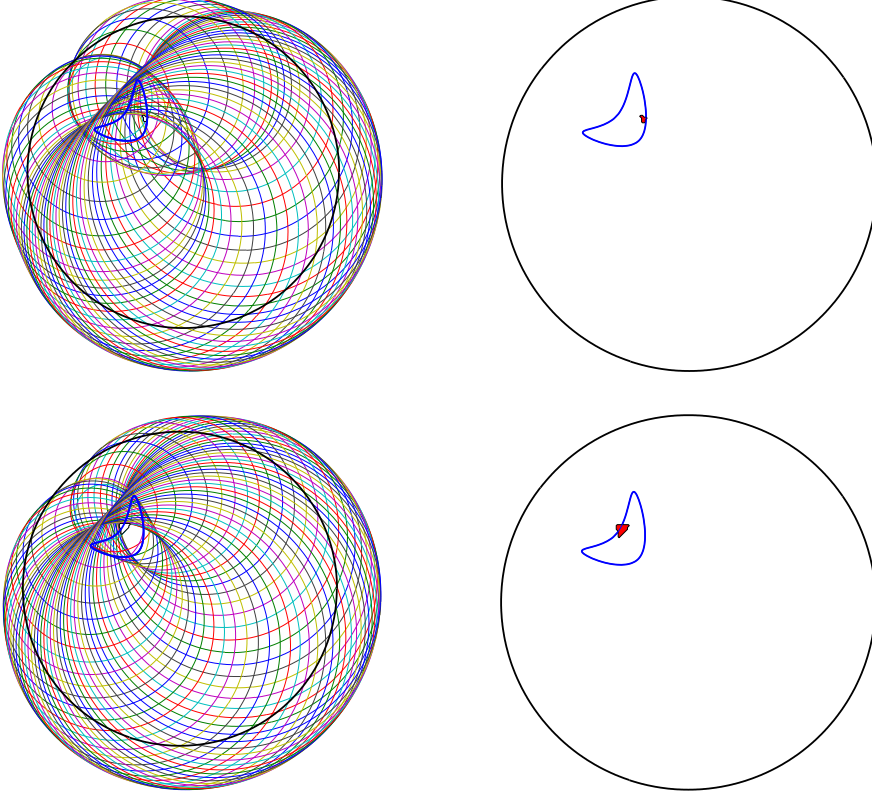


FIG. 6.3. Reconstructions of convex backscattering supports of the kite-shaped inclusion with 1% noise, using the conductivities $\sigma = 0$ (top line) and $\sigma = 0.5$ (bottom line), respectively (two different visualizations of the same result)

for every $r \in \mathbb{R}$. In particular, $v|_U \in C^\infty(U)/\mathbb{C}$.

Proof. Without loss of generality we may assume that s is an integer: Otherwise, we could work out the proof for some integer that is smaller than s , from which the result would follow for the original s as well. Throughout the following estimates, we denote the occurring constants generically by C .

Let $v \in H^s(U_0)$ be a representative of the quotient equivalence class under investigation, and let U_1 be a C^∞ -domain such that $\bar{U} \subset U_1$ and $\bar{U}_1 \subset U_0$. We choose a cut-off function $\varphi \in C_0^\infty(U_0)$ that is identically one in U_1 . The distribution $\tilde{v} = \varphi(v - c)$, $c \in \mathbb{C}$, satisfies the Dirichlet problem

$$\Delta \tilde{v} = F \quad \text{in } U_0, \quad \tilde{v} = 0 \quad \text{on } \partial U_0,$$

where $F = 2\nabla\varphi \cdot \nabla v + \Delta\varphi(v - c)$ is a compactly supported distribution in U_0 . Hence, it follows from [23, Chapter 2, Remark 7.2 and Definition 6.1] that

$$\begin{aligned} \|v\|_{H^{s+1}(U_1)/\mathbb{C}} &\leq \|v - c\|_{H^{s+1}(U_1)} \leq \|\tilde{v}\|_{H^{s+1}(U_0)} \leq C\|F\|_{H^{s-1}(U_0)} \\ &\leq C\left(\|v\|_{H^s(U_0)/\mathbb{C}} + \|v - c\|_{H^{s-1}(U_0)}\right), \end{aligned}$$

where the last step is a consequence of [23, Chapter 1, Proposition 12.1]. By taking

the infimum over $c \in \mathbb{C}$, we deduce that

$$\|v\|_{H^{s+1}(U_1)/\mathbb{C}} \leq C\|v\|_{H^s(U_0)/\mathbb{C}}.$$

After choosing another auxiliary domain U_2 , with $\overline{U} \subset U_2$ and $\overline{U}_2 \subset U_1$, the same line of reasoning gives the estimate

$$\|v\|_{H^{s+2}(U_2)/\mathbb{C}} \leq C\|v\|_{H^{s+1}(U_1)/\mathbb{C}} \leq C\|v\|_{H^s(U_0)/\mathbb{C}}.$$

Since this argument may be repeated as often as necessary, the proof is complete. \square

Next, we move on to consider the unique solvability of the forward problem (2.1).

THEOREM A.2. *Problem (2.1) has a unique solution in \mathcal{H}_s .*

Proof. Let $f \in H_\diamond^s(T)$, $s \in \mathbb{R}$, be the current pattern for (2.1) and (2.6). According to [23, Chapter 2, Remark 7.2], problem (2.6) has a unique solution $u_0 \in H^{s+3/2}(D)/\mathbb{C}$, which satisfies the estimate

$$\|u_0\|_{H^{s+3/2}(D)/\mathbb{C}} \leq C\|f\|_{H^s(T)}. \quad (\text{A.1})$$

Moreover, due to Lemma A.1, u_0 is smooth in the interior of D and thus $u_0 \in (H^{s+3/2}(D) \cap H_{\text{loc}}^1(D))/\mathbb{C} \subset \mathcal{H}_s$, with \mathcal{H}_s introduced in (2.3). We fix a simply connected C^∞ -domain Ω so that $\overline{\Sigma} \subset \Omega$ and $\overline{\Omega} \subset D$, and introduce a cut-off function $\varphi \in C_0^\infty(D)$ that is identically one in Ω . Furthermore, we let Ω_0 be another simply connected C^∞ -domain such that $\text{supp } \varphi \subset \Omega_0$ and $\overline{\Omega}_0 \subset D$. We denote the boundaries of Ω and Ω_0 by Γ and Γ_0 , respectively, and let their unit normals point out of the respective domains.

Let us consider the variational problem

$$\int_D \sigma \nabla w \cdot \nabla \overline{v} \, dx = \int_D \sigma \nabla u_0 \cdot \nabla (\overline{\varphi v}) \, dx \quad \text{for every } v \in H^1(D)/\mathbb{C}, \quad (\text{A.2})$$

and show that it has a unique solution $w \in H^1(D)/\mathbb{C}$; our ultimate goal is to prove that $u_0 - w$ is the solution of (2.1). First of all, it is easy to see that the left-hand side of (A.2) defines a bounded and coercive sesquilinear form from $H^1(D)/\mathbb{C} \times H^1(D)/\mathbb{C}$ to \mathbb{C} (cf. [13, Lemma 2.5]). Let us denote the antilinear functional defined by the right-hand side of (A.2) by $A : H^1(D)/\mathbb{C} \rightarrow \mathbb{C}$ and show that it is well defined and bounded. To start with, note that

$$A(1) = \int_{\Omega_0 \setminus \overline{\Omega}} \nabla u_0 \cdot \nabla \overline{\varphi} \, dx = - \int_\Gamma \frac{\partial u_0}{\partial \nu} \, ds = 0,$$

where the second step follows from Green's identity and the last one from the Divergence Theorem. This shows that A does not see the constant and is thus well defined. In order to deduce the continuity, we estimate with the help of the Schwarz inequality as follows:

$$\begin{aligned} |A(v)| &= |A(v - c)| \leq \|\sigma \nabla u_0\|_{L^2(\Omega_0)} \|\nabla(\varphi(v - c))\|_{L^2(\Omega_0)} \\ &\leq C(\sigma, \varphi) \|u_0\|_{H^1(\Omega_0)/\mathbb{C}} \|v - c\|_{H^1(\Omega_0)}. \end{aligned} \quad (\text{A.3})$$

By taking the infimum over $c \in \mathbb{C}$, it follows that

$$|A(v)| \leq C\|u_0\|_{H^1(\Omega_0)/\mathbb{C}} \|v\|_{H^1(\Omega_0)/\mathbb{C}} \leq C\|f\|_{H^s(T)} \|v\|_{H^1(D)/\mathbb{C}},$$

where the second step is a consequence of Lemma A.1 and (A.1). Now, the unique solvability of (A.2) follows from the Lax-Milgram lemma, cf., e.g., Dautray and Lions [3, p. 368], which also gives the estimate

$$\|w\|_{H^1(D)/\mathbb{C}} \leq C\|f\|_{H^s(T)}. \quad (\text{A.4})$$

Observe that the solution $w \in H^1(D)/\mathbb{C}$ does not depend on φ because a simple application of Green's identity reveals that the value of the functional A is independent of the particular choice of this cut-off function.

Choosing $v \in C_0^\infty(D)$ in (A.2) and using the distributional definition of the divergence (cf. [3, p. 467, Definition 8]) together with the interior regularity of u_0 , it follows that

$$\begin{aligned} \langle \nabla \cdot (\sigma \nabla w), v \rangle &= - \int_D \sigma \nabla w \cdot \nabla \bar{v} \, dx \\ &= \int_D \sigma \nabla u_0 \cdot \nabla((1 - \bar{\varphi})\bar{v}) \, dx - \int_D \sigma \nabla u_0 \cdot \nabla \bar{v} \, dx \\ &= \int_{D \setminus \bar{\Omega}} \nabla u_0 \cdot \nabla((1 - \bar{\varphi})\bar{v}) \, dx + \langle \nabla \cdot (\sigma \nabla u_0), v \rangle, \end{aligned}$$

where the first term on the right-hand side is zero due to Green's identity since u_0 is harmonic and $(1 - \varphi)v$ vanishes on Γ and in some neighborhood of T . In consequence,

$$\nabla \cdot (\sigma \nabla w) = \nabla \cdot (\sigma \nabla u_0) \quad \text{in } D$$

in the distributional sense; in particular, w is harmonic away from the support of $\sigma - 1$. Moreover, applying test functions that are supported away from Ω_0 in (A.2), it follows by a common variational argument that the Neumann trace of w vanishes on T . Altogether, we have thus deduced that $u = u_0 - w \in \mathcal{H}_s$ is a solution of (2.1), and the combination of (A.1) and (A.4) gives

$$\|u\|_{H^{\min\{1, s+3/2\}}(D)/\mathbb{C}} \leq C\|f\|_{H^s(T)}. \quad (\text{A.5})$$

The function u constructed above is, in fact, the unique solution of (2.1) in \mathcal{H}_s . To prove this, let $h \in \mathcal{H}_s$ be the difference of two solutions to (2.1). In particular, h satisfies the boundary value problem

$$\Delta h = 0 \quad \text{in } D \setminus \bar{\Omega}, \quad \frac{\partial}{\partial \nu} h = 0 \quad \text{on } T, \quad h = g \quad \text{on } \Gamma,$$

for some $g \in H^{1/2}(\Gamma)/\mathbb{C}$, due to the trace theorem and the interior regularity of the distributions in \mathcal{H}_s . As a consequence, $h|_{D \setminus \bar{\Omega}} \in H^1(D \setminus \bar{\Omega})/\mathbb{C}$, cf. [23, Chapter 2, Remark 7.2], and we deduce that $h \in H^1(D)/\mathbb{C}$. Since h satisfies (2.1) with $f = 0$, it now follows from the Lax-Milgram lemma that h is a constant, i.e., the zero element of \mathcal{H}_s . Hence, we have established the unique solvability of (2.1). \square

To conclude this appendix, we show that the various operators introduced in Sections 2 and 3 are bounded.

THEOREM A.3. *The linear operators defined by (2.5), (2.7), (3.3), (3.7) and (3.6) are well defined and bounded.*

Proof. We start with the Neumann-to-Dirichlet operators (2.5) and (2.7). Let $f \in H_\diamond^s(T)$ be arbitrary and denote the corresponding solutions of (2.1) and (2.6) by $u \in \mathcal{H}_s$ and $u_0 \in H^{s+3/2}(D)/\mathbb{C}$, respectively. Furthermore, choose Ω and Γ as

in Section 3, and let U and U_0 be as in Lemma A.1 and such that $\Gamma \subset U$ and $\overline{U_0} \subset D \setminus \overline{\Sigma}$. As u is harmonic in $D \setminus \overline{\Sigma}$, it follows from [23, Chapter 2, Remark 7.2] and the appropriate trace theorem (cf. [23, Chapter 2, Theorems 6.5 and 7.3] and the related remarks) that

$$\|u\|_{H^{s+1}(T)/\mathbb{C}} \leq C\|u\|_{H^{s+3/2}(D \setminus \overline{\Omega})/\mathbb{C}} \leq C\left(\|f\|_{H^s(T)} + \|\partial u / \partial \nu\|_{H^s(\Gamma)}\right). \quad (\text{A.6})$$

Furthermore, with the help of the trace theorems in [23], Lemma A.1 and (A.5), we see that

$$\|\partial u / \partial \nu\|_{H^s(\Gamma)} \leq C\|u\|_{H^{s+3/2}(U)/\mathbb{C}} \leq C\|u\|_{H^{\min\{1, s+3/2\}}(U_0)/\mathbb{C}} \leq C\|f\|_{H^s(T)}.$$

Combining this with (A.6), we finally get

$$\|u\|_{H^{s+1}(T)/\mathbb{C}} \leq C\|f\|_{H^s(T)}.$$

Since $w = u_0 - u$ has vanishing Neumann trace on T , the same line of reasoning, together with (A.4), shows also that

$$\begin{aligned} \|w\|_{H^r(T)/\mathbb{C}} &\leq C\|\partial w / \partial \nu\|_{H^{r-1}(\Gamma)} \leq C\|w\|_{H^{r+1/2}(U)/\mathbb{C}} \\ &\leq C\|w\|_{H^1(U_0)/\mathbb{C}} \leq C\|f\|_{H^s(T)} \end{aligned}$$

for any $r \in \mathbb{R}$. These last two estimates establish the continuity of the operators (2.5) and (2.7) for every $s \in \mathbb{R}$. The boundedness of the operators (3.3) and (3.7) can be proved using similar techniques.

To complete the proof, we show that the extended operator (3.6) is well defined and bounded. Let $h \in (H^1(\Omega)/\mathbb{C}^m) \oplus (H^1(D \setminus \overline{\Omega})/\mathbb{C})$ be the solution of (3.5) for $\psi \in H^{1/2}(\Gamma)/\mathbb{C}^m$, and $h_0 \in (H^1(\Omega)/\mathbb{C}^m) \oplus (H^1(D \setminus \overline{\Omega})/\mathbb{C})$ be the corresponding solution when σ is replaced by 1. Abusing the notation slightly, we pick a representative of the equivalence class $h - h_0$ having continuous Dirichlet trace over Γ , and continue denoting it by $h - h_0$. Since the Neumann trace of $h - h_0$ is also continuous over Γ , it follows that $h - h_0$ is harmonic and, in particular, smooth in the whole of $D \setminus \overline{\Sigma}$. Hence, the same argument as for u and w above, gives us the estimate

$$\left\| \frac{\partial}{\partial \nu} (h - h_0) \right\|_{H^{-s}(\Gamma)} \leq C\|h - h_0\|_{H^1(U_0)/\mathbb{C}} \leq C\|\psi\|_{H^{1/2}(\Gamma)/\mathbb{C}^m}$$

for any $s \leq 1/2$, where the last step follows from the continuous dependence of the solution on the data in (3.5) (cf., e.g., [18, 10]). As a consequence, F maps $H^{1/2}(\Gamma)/\mathbb{C}^m$ continuously to $H_{\infty}^{-s}(\Gamma)$ for any $s \in \mathbb{R}$, and thus the dual operator of F maps $H^s(\Gamma)/\mathbb{C}^m$ continuously to $H_{\infty}^{-1/2}(\Gamma)$. Since $F : H^{1/2}(\Gamma)/\mathbb{C}^m \rightarrow H_{\infty}^{-1/2}(\Gamma)$ and its dual operator coincide, it follows from interpolation theory, cf., e.g., Triebel [26], that F has an extension to a bounded operator

$$F : H^{s/2+1/4}(\Gamma)/\mathbb{C}^m \rightarrow H_{\infty}^{-s/2-1/4}(\Gamma),$$

compare, for example, the proof of Theorem 2.1 in [14]. By choosing s appropriately we see that the extension of F given in (3.6) is bounded. \square

- [1] Brühl, M.: Explicit characterization of inclusions in electrical impedance tomography. *SIAM J. Math. Anal.* **32**, 1327–1341 (2001)
- [2] Bryan, K.: Numerical recovery of certain discontinuous electrical conductivities. *Inverse Problems* **7**, 827–840 (1991)
- [3] Dautray, R., Lions, J-L.: *Mathematical Analysis and Numerical Methods for Science and Technology*. Vol. 2, Springer, Berlin (1988)
- [4] Gebauer, B.: The factorization method for real elliptic problems. *Z. Anal. Anwendungen* **25**, 81–102 (2006)
- [5] Haddar, H., Kusiak, S., Sylvester, J.: The convex back-scattering support. *SIAM J. Appl. Math.* **66**, 591–615 (2005)
- [6] Hanke, M.: On real-time algorithms for the location search of discontinuous conductivities with one measurement. *Inverse Problems* **24**, 045005 (16pp) (2008)
- [7] Hanke, M., Hyvönen, N., Lehn, M., Reusswig, S.: Source supports in electrostatics. *BIT* **48**, 245–264 (2008)
- [8] Hanke, M., Hyvönen, N., Reusswig, S.: Convex source support and its application to electric impedance tomography. *SIAM J. Imaging Sci.* **1**, 364–378 (2008)
- [9] Hanke, M., Hyvönen, N., Reusswig, S.: An inverse backscatter problem for electric impedance tomography. *SIAM J. Math. Anal.* **41**, 1948–1966 (2009).
- [10] Hanke, M., Kirsch, A.: Sampling Methods, in O. Scherzer, ed., *Handbook of Mathematical Methods in Imaging*, Springer, New York, to appear.
- [11] Henrici, P.: *Applied and Computational Complex Analysis*. Vol. 1, Wiley, New York (1974)
- [12] Hettlich, F., Rundell, W.: The determination of a discontinuity in a conductivity from a single boundary measurement. *Inverse Problems* **14**, 67–82 (1998)
- [13] Hyvönen, N.: Complete electrode model of electrical impedance tomography: Approximation properties and characterization of inclusions. *SIAM J. Appl. Math.* **64**, 902–931 (2004)
- [14] Hyvönen, N.: Application of a weaker formulation of the factorization method to the characterization of absorbing inclusions in optical tomography. *Inverse Problems* **21**, 1331–1343 (2005)
- [15] Hyvönen, N.: Application of the factorization method to the characterization of weak inclusions in electrical impedance tomography. *Adv. in Appl. Math.* **39**, 197–221 (2007)
- [16] Ito, K., Kunisch, K., Li, Z.: Level-set function approach to an inverse interface problem. *Inverse Problems* **17**, 1225–1242 (2001)
- [17] Kang, H., Seo, J. K., Sheen, D.: Numerical identification of discontinuous conductivity coefficients. *Inverse Problems* **13**, 113–123 (1997)
- [18] Kirsch, A.: The factorization method for a class of inverse elliptic problems. *Math. Nachr.* **278**, 258–277 (2005)
- [19] Kress, R.: Inverse Dirichlet problem and conformal mapping. *Math. Comput. Simulation* **66**, 255–265 (2004)
- [20] Kress, R., Kühn, L.: Linear sampling methods for inverse boundary value problems in potential theory. *Appl. Numer. Math.* **43**, 161–173 (2002)
- [21] Kress, R., Rundell, W.: Nonlinear integral equations and the iterative solution for an inverse boundary value problem. *Inverse Problems* **21**, 1207–1223 (2005)
- [22] Kusiak, S., Sylvester, J.: The scattering support. *Comm. Pure Appl. Math.* **56**, 1525–1548 (2003)
- [23] Lions, J-L., Magenes, E.: *Non-Homogeneous Boundary Value Problems and Applications*. Vol. 1, Springer, Berlin (1972)
- [24] Rundell, W.: Recovering an obstacle and its impedance from Cauchy data. *Inverse Problems* **24**, 045003 (22pp) (2008)
- [25] Tutschke, W., Vasudeva, H. L.: *An Introduction to Complex Analysis: Classical and Modern Approaches*. Chapman & Hall, Boca Raton (2005)
- [26] H. Triebel, H.: *Interpolation Theory, Function Spaces, Differential Operators*. VEB Deutscher Verlag der Wissenschaften, Berlin (1978)